DEVELOPMENTS ON EXPLICIT ALGEBRAIC REYNOLDS STRESS MODELS

Hervé Bézard
Aerodynamics and Energetics Modeling Department, ONERA
BP 4025. 2, av. E. Belin, 31055 Toulouse, France
Herve.Bezard@onecert.fr

ABSTRACT

An explicit algebraic Reynolds stress model is extended to the wall. It is shown analytically how to reproduce the near-wall behaviour of Reynolds stresses through the variation of the model constants. A complete model is proposed and applied to two-dimensional boundary layers in adverse pressure gradient. The extension to three-dimensional flows is simply obtained and no further wall damping is needed. The model is applied also to rotating pipe flows.

INTRODUCTION

Explicit Algebraic Reynolds Stress Models (EARSM) offer a great potential for CFD applications in industrial flows with strong effects of adverse pressure gradients or system rotation. Indeed they improve the predictions of Reynolds stress anisotropies which are important in such flows but they allow to keep the traditional two-equation turbulence model resolution in CFD codes with no addition of new transport equation.

For two-dimensional mean flows, an exact solution of the algebraic Reynolds stress equation has been obtained by Wallin & Johansson (2000) who proposed an extension for wall regions. Damping functions of van Driest type were applied directly on the components of the anisotropy tensor. This paper deals with some developments made on EARSM models based on Wallin & Johansson expression. The near-wall extension is made by introducing directly the damping functions in the modelling constants, following some recent developments on RSM models by Shima (1997). An interesting feature of this approach is that the theoretical behaviour of the anisotropy components in the sub-layer region can be prescribed exactly, ensuring the two-component turbulence behaviour at the wall. The wall damping functions are expressed in terms of the turbulence Reynolds number Re_y which is preferable to the normalised wall-distance y^+ to avoid a poor behaviour close to the separation point.

The new EARSM model is applied in relation with a two-layer $k/k-\varepsilon$ model in APG two-dimensional boundary layer flows and in rotating pipe flows where a three-dimensional EARSM formulation is needed.

EARSM FORMULATION

The EARSM expression is based on the algebraic equation for the Reynolds stress anisotropy tensor ($\underline{\underline{\mathbf{b}}} = \underline{\underline{\tau}}/2k - 1/3\underline{\underline{\mathbf{I}}}$) obtained from the full Reynolds stress transport equation assuming local equilibrium and neglecting diffusion:

$$(2\underline{\underline{\mathbf{b}}} + 2/3\underline{\underline{\mathbf{I}}})(P-\varepsilon) = \underline{\underline{\mathbf{P}}} - \underline{\underline{\varepsilon}} + \underline{\underline{\mathbf{\Pi}}} \quad (1)$$

The dissipation tensor $\underline{\underline{\varepsilon}}$ is assumed to be isotropic so that $\underline{\underline{\varepsilon}} = 2/3\varepsilon\underline{\underline{\mathbf{I}}}$. The pressure strain tensor $\underline{\underline{\mathbf{\Pi}}}$ is assumed to be linear with respect to the anisotropy tensor:

$$\begin{aligned} \underline{\underline{\mathbf{\Pi}}}/\varepsilon &= -2C_1\underline{\underline{\mathbf{b}}} - 2C_1'P/\varepsilon\underline{\underline{\mathbf{b}}} + C_2\underline{\underline{\mathbf{S}}} \\ &+ C_3(\underline{\underline{\mathbf{b}}}.\underline{\underline{\mathbf{S}}} + \underline{\underline{\mathbf{S}}}.\underline{\underline{\mathbf{b}}} - 2/3tr\{\underline{\underline{\mathbf{b}}}.\underline{\underline{\mathbf{S}}}\}\underline{\underline{\mathbf{I}}}) \\ &- C_4(\underline{\underline{\mathbf{b}}}.\underline{\underline{\mathbf{\Omega}}} - \underline{\underline{\mathbf{\Omega}}}.\underline{\underline{\mathbf{b}}}) \end{aligned} \quad (2)$$

where $\underline{\underline{\mathbf{S}}}$ and $\underline{\underline{\mathbf{\Omega}}}$ are respectively the mean strain tensor and the mean rotation tensor both normalized by the turbulence time scale $\tau = k/\varepsilon$. This form is the most general linear form and contains any linear pressure strain model as the LRR model from Launder *et al.* (1975) or the linear SSG model used by Gatski & Speziale (1993).

The solution for $\underline{\underline{\mathbf{b}}}$ is sought as a combination of independent tensor groups made with the velocity gradient tensors $\underline{\underline{\mathbf{S}}}$ and $\underline{\underline{\mathbf{\Omega}}}$ following the approach proposed by Pope (1975). Three tensorial groups are independent for two-dimensional flows whereas there are ten groups for three-dimensional flows in the most general case. However by a suitable choice of the modelling constants of the pressure strain expression, the expression for $\underline{\underline{\mathbf{b}}}$ can be reduced respectively to two and five groups as shown by Wallin & Johansson (2000). For two-dimensional flows the anisotropy tensor is sought as:

$$\underline{\underline{\mathbf{b}}} = \beta_1 \underline{\underline{\mathbf{S}}} + \beta_2 (\underline{\underline{\mathbf{S}}}^2 - 1/3\eta_1 \underline{\underline{\mathbf{I}}}) + \beta_3 (\underline{\underline{\mathbf{S}}}\underline{\underline{\mathbf{\Omega}}} - \underline{\underline{\mathbf{\Omega}}}\underline{\underline{\mathbf{S}}}) \quad (3)$$

where $\eta_1 = tr(\underline{\underline{\mathbf{S}}}^2)$ and $\eta_2 = tr(\underline{\underline{\mathbf{\Omega}}}^2)$. When the anisotropy expression (3) is introduced into the algebraic equation (1), the expression of the β_i coefficients is found as function of the velocity gradient invariants and P/ε. An equation for $P/\varepsilon = -2tr(\underline{\underline{\mathbf{bS}}})$ is then obtained, which is of the third degree for two-dimensional flows and has consequently an explicit solution. For three-dimensional flows the equation is of the sixth degree and only an approximate solution for P/ε can be found. Otherwise the expression is implicit and the solution has to be found through an iterative procedure, which is not suitable as it may increase the computational effort and may lead to non-physical solutions.

The EARSM model needs the knowledge of the normalised velocity tensors $\underline{\underline{\mathbf{S}}}$ and $\underline{\underline{\mathbf{\Omega}}}$ and of the five constants C_1, C_1', C_2, C_3 and C_4 which have to be prescribed either theoretically or empirically. The C_1 constant can be found experimentally considering the return to isotropy of turbulent flow when velocity gradients are suppressed. The values obtained lie usually between 1.5 and 2.5 depending upon the experiments. The C_1' constant comes from the SSG model and has no theoretical basis. It can thus be set to zero for the sake of simplicity. The C_2 constant can be found theoretically considering the Rapid Distortion Theory limit and takes the value of 4/5. The C_3 and C_4 constants can be obtained through experiments. The LRR pressure strain model respects the normalisation constraint so that C_3 and C_4 are not independent, which is not the case for the linear SSG model.

The approach proposed here follows the SSG model where C_3 and C_4 are calibrated independently using equilibrium shear flow data. The objective is to reproduce anisotropy values found in experiments or DNS: homogeneous shear flow and logarithmic law in boundary layer or plane channel flows. For these flows, there are three independent anisotropy components. As two constants have already be prescribed ($C_1' = 0$ and $C_2 = 4/5$), the three others (C_1, C_3 and C_4) can be obtained from only one experiment or DNS result. However it is preferable to obtain a set of constants which gives the best result over a family of referenced data. By minimising the rms deviation between the theoretical and the data, the following values were obtained:

$$\begin{cases} C_{1_{eq}} = 1.5 & C'_{1_{eq}} = 0 \qquad C_{2_{eq}} = 4/5 \\ C_{3_{eq}} = 1.6 & C_{4_{eq}} = 1.08 \end{cases} \quad (4)$$

As shown in fig. 1, they reproduce nearly the same results as the Gatski & Speziale (GS) model without the need of the C_1' constant. They also differ from the values of Wallin & Johansson (WJ) but provide a good behaviour for all anisotropy components compared to the existing data for equilibrium flows.

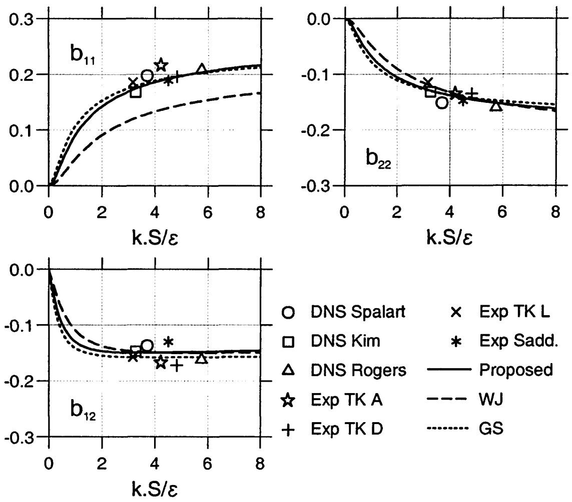

Figure 1: Evolution of anisotropy components with total shear rate $k.S/\varepsilon$ in equilibrium shear flows - Comparison of EARSM predictions with DNS and experiments.

NEAR-WALL EXTENSION

First of all it is important to limit the turbulent time scale $\tau = k/\varepsilon$ which scales the velocity gradients when approaching the wall as this quantity goes to zero. Physically the turbulent time scale is limited by the Kolmogorov time scale and following Durbin (1993) we adopt the expression:

$$\tau = \max(k/\varepsilon, C_\tau \sqrt{\nu/\varepsilon}) \quad \text{with} \quad C_\tau = 6 \quad (5)$$

The near-wall extension of the homogeneous expression of the EARSM is obtained by introducing wall damping functions directly into the modelling constants, following recent approaches proposed in second-moment closures such as in the RSM model of Shima (1997). There are two different behaviours in the near-wall region: in the sub-layer region ($y^+ < 3$) the convection and the production of turbulence are neglictible and the molecular diffusion equilibrates the dissipation; in this region the turbulence is almost in a two-component state. In the buffer-layer region ($3 < y^+ < 100$) the convection is still neglictible but the other terms are of the same order. Because the extent and the physics of both regions are very different, two different dampings were introduced: one active in the sub-layer and the second active from the sub-layer up to the logarithmic region. Consequently each constant is sought as:

$$C_i = C_{i_0}(1 - f_i) + C_{i_{eq}} f_b \qquad (6)$$

where C_{i_0} is the value of the constant at the wall, f_i is a wall damping function which acts only in the sub-layer region and f_b is a wall damping function which acts also in the buffer region up to the logarithmic region (f_i and f_b lie between 0 at the wall and 1). The constants are thus continuously evolving from their value at the wall C_{i_0} to their value in the logarithmic region where they take the equilibrium value $C_{i_{eq}}$.

Close to the wall in the sub-layer region, the theoretical behaviour of the anisotropy components as a function of the normalised wall-distance y^+ is known to be:

$$\begin{cases} b_{11} &= b_{11_0} + ry^+ + O(y^{+2}) \\ b_{22} &= -2/3 + O(y^{+2}) \\ b_{12} &= sy^+ + O(y^{+2}) \end{cases} \qquad (7)$$

where b_{11_0}, r and s can be obtained from DNS. Introducing expression (6) in the EARSM formulation and making a Taylor expansion with respect to y^+, the behaviour of the anisotropy predicted by the model is obtained. Thus by comparison with the expected behaviour (7), the values of C_{i_0} and the y^+ developments of the f_i functions are obtained. It is first found that:

$$\begin{cases} C_{2_0} = C_{4_0}^2 & C_{3_0} = C_{4_0} \\ C_{4_0} = 4/3 - 2b_{11_0} & \end{cases} \qquad (8)$$

whereas C_{1_0} is not determined. A way to prescribe this value is to assume the realizability of the slow part of the pressure strain tensor which imposes $C_{1_0} = 1$. To obtain the other values it is necessary to prescribe the value of b_{11_0}. Based on DNS we assume that $b_{11_0} = 1/3$. The C_{i_0} then takes the values:

$$C_{1_0} = 1,\ C_{2_0} = 4/9,\ C_{3_0} = 2,\ C_{4_0} = 2/3 \qquad (9)$$

The y^+-behaviour of the f_i functions is:

$$\begin{cases} f_1 = \alpha_1 y^{+2} + O(y^{+3}) \\ f_4 = \alpha_4 y^+ + O(y^{+2}) \\ f_2 = f_3 = 2\alpha_4 y^+ + O(y^{+2}) \end{cases} \qquad (10)$$

The f_1 function which damps the C_1 constant in the sub-layer region behaves quite differently from the other functions as it is at least parabolic in y^+ whereas the others are linear in y^+. To restrict the number of functions used, it can be chosen as the same as the buffer-layer damping function f_b which behaves as y^{+2} in the sub-layer to avoid the interaction with the sub-layer linear functions f_2, f_3 and f_4. The slope α_4 can be determined with the help of DNS. However this analysis showed that it is difficult to obtain the correct behaviour for the b_{12} term by the use of classical functions (exponential, hyperbolic...). A simple solution is then to also damp the term $(P/\varepsilon)_{eq}$ calculated by the equilibrium EARSM expression as: $P/\varepsilon = (P/\varepsilon)_{eq}.f_p$ where f_p is an additional wall damping function which acts in the buffer region as f_b. It can be shown that f_p has to be linear in y^+ in the sub-layer region.

The buffer layer function f_b could be obtained in a formal way by solving the transport equation for the turbulent scales assuming the shape of the velocity profile is known. However in this paper the f_b function was determined through the help of DNS data. All the damping functions f_i, f_b and f_p were chosen as simple exponential functions based on the turbulent Reynolds number $Re_y = y\sqrt{k}/\nu$. This approach has been validated on the flat plate boundary layer DNS of Spalart (1988) using the U, k and ε profiles of the DNS. The results are presented in fig. 2.

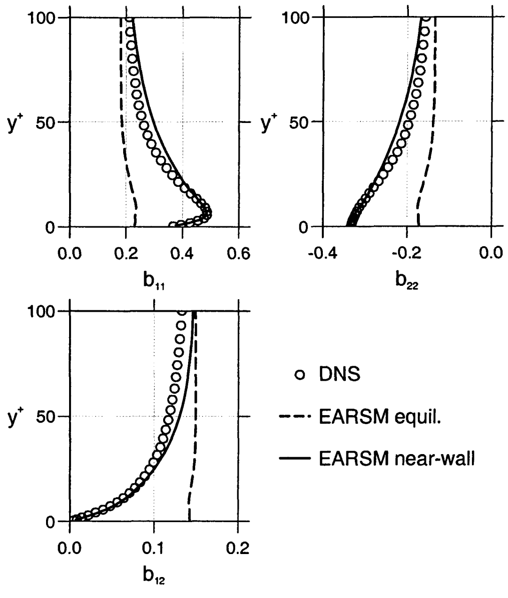

Figure 2: Evolution of anisotropy components with normalised wall distance - Flat plate boundary layer $R_\theta = 1410$ - Comparison of EARSM predictions with the DNS of Spalart (1988).

As a comparison the predictions obtained with the EARSM expression without any wall damping is also presented in the figure. It shows that the equilibrium expression is not able to reproduce the correct anisotropy field in the wall region, even if the velocity and turbulent fields are correct and even if the EARSM adjusts itself in a more natural way to the near-wall flow than a two-equation turbulence model based on Boussinesq constitutive relation. The comparison of the anisotropy components between the DNS and the EARSM prediction is quite correct on the b_{11} and b_{22} terms, but it could be further improved on the b_{12} term by the use of more complex functions. However considering future CFD applications it is important to keep simple and robust expressions for the damping functions.

LENGTH SCALE EQUATION

Because the EARSM modifies the constitutive relation between the Reynolds stresses and the velocity gradients, the length scale equation of a two-equation model is supposed to behave differently when it is used in association with an EARSM. A good approach would be to develop the length scale equation taking into account the EARSM expression from the beginning. However this point is not presented in this paper but will be addressed in future studies.

Here the proposed EARSM was used in association with an existing two-layer $k/k-\varepsilon$ model. The inner k-model is the Chen & Patel model (1988) and the outer $k-\varepsilon$ model is the high-Reynolds number Launder-Sharma model (1974). The blended model switches from the inner model to the outer model when the turbulent Reynolds number Re_y reaches a given value (usually 250) in the logarithmic region. The diffusion model for k and ε equations is the Daly & Harlow model (1970) where the diffusion constants c_k and c_ε were kept to their initial values of respectively 0.25 and 0.15. There is an interest to use this gradient diffusion model rather than a classical diffusion model because the full Reynolds stress tensor is known through the EARSM expression and one may expect an improvement to use a more accurate model. Assuming the production-to-dissipation equilibrium in the logarithmic region, a relation is obtained between the modelling constants of the ε-equation and the EARSM formulation. With the numerical values given in (4), we obtain the relation:

$$C_{\varepsilon_2} - C_{\varepsilon_1} \approx 15\kappa^2 c_\varepsilon \qquad (11)$$

Keeping the classical value $C_{\varepsilon_2} = 1.92$ and assuming the value of von Kármán constant $\kappa = 0.41$, we obtain $C_{\varepsilon_1} = 1.54$, which is close to the standard value. The EARSM near-wall extension has to be tuned specifically to be used with the k-equation model as it does not reproduce the same turbulent field as in the DNS data. The final form of the damping functions are:

$$\left\{\begin{array}{l} f_b = 1 - exp(-\alpha_b Re_y) \\ f_4 = 1 - exp(-\sqrt{\alpha_4 Re_y}) \\ f_p = 1 - exp(-\sqrt{\alpha_p Re_y}) \\ f_1 = f_b \quad f_2 = f_4^2 \quad f_3 = f_4 \\ \alpha_b = 0.005 \quad \alpha_4 = 0.1 \quad \alpha_p = 0.03 \end{array}\right. \qquad (12)$$

APPLICATION TO APG BOUND. LAYERS

The proposed model was first applied in APG boundary layer flows. Fig. 3 presents the longitudinal evolution of the friction coefficient in the Samuel & Joubert (1974) experiment.

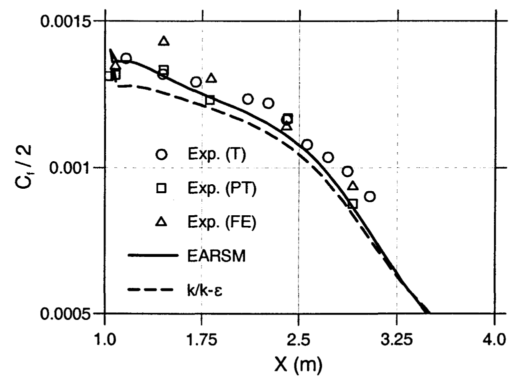

Figure 3: Evolution of the friction coefficient - Comparison of the EARSM and the two-layer $k/k-\varepsilon$ model predictions with the experiment of Samuel & Joubert (1974).

The EARSM is compared to the initial two-layer model and to the experiments. The EARSM shows a good agreement with the data and a better evolution than the original model. However the differences are quite small because the original two-layer model behaves well in APG flows. The velocity profiles are presented in fig. 4. In the wake part of the boundary layer the EARSM performs better than the $k-\varepsilon$ model. This is a result of the modification of the constitutive relation as the EARSM is able to maintain the level of anisotropy in this region while P/ε is varying, contrarily to a classical two-equation model.

The model was then applied to the experiment of Skåre & Krogstad (1994). Fig. 5

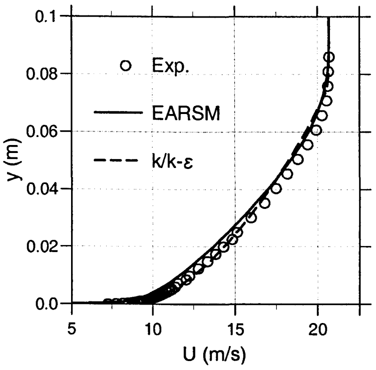

Figure 4: Velocity profile at $x = 3.04m$ - Comparison of the EARSM and the two-layer $k/k - \varepsilon$ model predictions with the experiment of Samuel & Joubert (1974).

presents the longitudinal evolution of the friction coefficient. In this case the EARSM provides less better comparison to the experiments than the original two-layer model. In the original model the length scale is imposed in the near-wall region and even in a large part of the logarithmic region. However the EARSM formulation interacts with the length scale and modifies its good behaviour in the inner region.

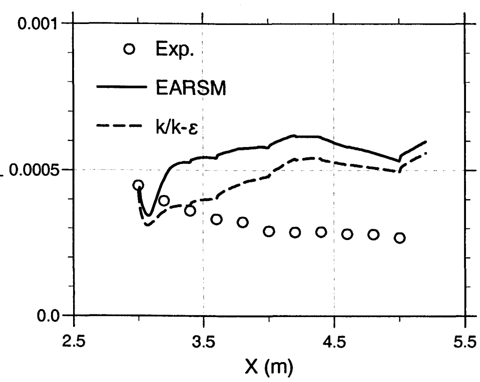

Figure 5: Evolution of the friction coefficient - Comparison of the EARSM and the two-layer $k/k - \varepsilon$ model predictions with the experiment of Skåre & Krogstad (1994).

The velocity profile presented in fig. 6 shows that the outer part of the boundary layer is better predicted with the EARSM than with the original two-layer model, as noticed before. However a logarithmic plot of the velocity profile would show that the EARSM underestimates the logarithmic law slope. In this case the interaction with the length scale is not positive. The result is that even if the wake region is well predicted, the deterioration of the logarithmic law slope provides too low C_f values. This result shows that the length scale equation has to be developed in relation with the EARSM expression to get good results in APG flows.

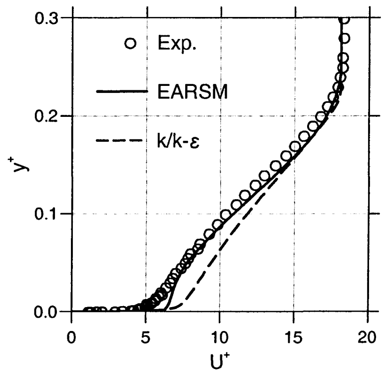

Figure 6: Velocity profile at $x = 5m$ - Comparison of the EARSM and the two-layer $k/k - \varepsilon$ model predictions with the experiment of Skåre & Krogstad (1994).

APPLICATION TO THE ROTATING PIPE

Applying the EARSM model to three-dimensional flows does not need any further developments as the near-wall damping is contained into the modelling constants. When approaching the wall, every component of the anisotropy tensor is damped naturally as P/ε is. The major problem comes from the approximation made on the P/ε estimation as no explicit solution for this term exists for three-dimensional flows. The ratio is thus estimated from a perturbation of the two-dimensional solution, following Wallin & Johansson (2000). For this type of flow the classical Boussinesq models fail to predict the modification of the flow with the rotation.

The EARSM predicts the good behaviour as presented in fig. 7 and fig. 8 which show respectively the axial and azimuthal velocity components in the experiment of Imao *et al.* (1996) for different rotation numbers. Due to the particular choice of the modelling constants, the EARSM expression (3) contains nine different tensorial groups for three-dimensional flows, but no numerical weakness behaviour was noticed in the computation. The EARSM compares well to the experiment on both velocity components. It gives the correct effect with the rotation: the maximum axial velocity component at the center of the pipe increases with the rotation number (fig. 7) and the azimuthal component moves away from the linear profile (fig. 8). However this last behaviour is less pronounced with the EARSM than in the experiments.

CONCLUSION

A novel approach was proposed to extend an EARSM model to near-wall regions by applying wall damping functions directly on the

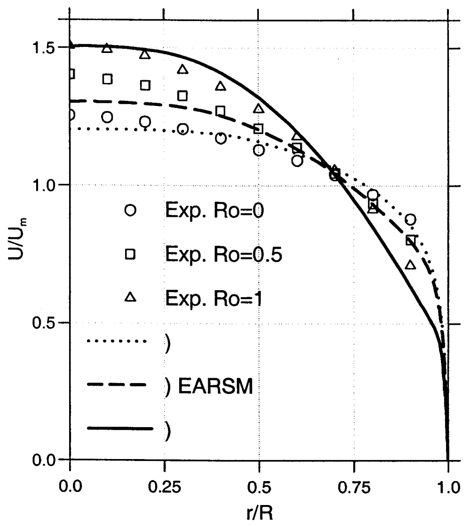

Figure 7: Axial velocity profile for the rotating pipe - Comparison of EARSM with the experiments of Imao *et al.* (1996) at different rotation numbers: Ro=0, 0.5, 1.

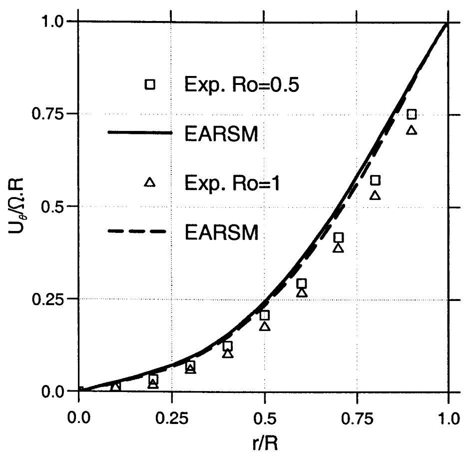

Figure 8: Azimuthal velocity profile for the rotating pipe - Comparison of EARSM with the experiments of Imao *et al.* (1996) at different rotation numbers: Ro= 0.5, 1.

modelling constants. The analysis of the sublayer region provides relations which served as a guide to build well-behaved functions. Applications to two-dimensional APG boundary layers in association with a two-layer $k/k-\varepsilon$ model proved that this approach was valid. The main interest is that the extension to three-dimensional flows, such as the rotating pipe flow, is straightforward and does not need any further developments. However the EARSM model could be further improved by developing a specific length scale determining equation in association with the EARSM formulation.

This work was developed within the framework of a Federating Research Project on Turbulence supported by ONERA. It was also developed in collaboration with Dassault-Aviation and was supported by the French Ministry of Defense through the Délégation Générale de l'Armement (DGA).

References

Chen H.C. and Patel, V.C., 1988, "Near-wall turbulence models for complex flows including separation", *AIAA Journal*, Vol. 26, No 6, pp. 641-648.

Daly, J. B. and Harlow, F. H., 1970, "Transport equations in turbulence", *The Physics of Fluids*, Vol. 13, No 11, pp. 2634-2649.

Gatski, T.B. and Speziale, C.G., 1993, "On explicit algebraic stress models for complex turbulent flows", *J. Fluid Mech.*, Vol. 254, pp. 59-78.

Imao, S., Itoh, M. and Harada, T., 1996, "Turbulent characteristics of the flow in an axially rotating pipe", *Int. J. of Heat and Fluid Flow*, Vol. 17, pp. 444-451.

Launder, B.E., Reece, G.J. and Rodi, W., 1975, "Progress in the development of a Reynolds-stress turbulence closure", *J. Fluid Mech.*, Vol. 68, pp. 537-566.

Launder, B.E. and Sharma, B.I., 1974, "Application of the energy-dissipation model of turbulence to the calculation of flow near a spinning disc", *Letters in Heat and Mass Transfer*, Vol. 1, pp. 131-138.

Pope, S.B., 1975, "A more general effective-viscosity hypothesis", *J. Fluid Mech.*, Vol. 72, pp. 331-340.

Samuel, A. E. and Joubert, P. M., 1974, "A boundary layer developing in an increasingly adverse pressure gradient", *J. Fluid Mech.*, Vol. 66, No 3, pp. 481-505.

Shima, N., 1997, "Low-Reynolds-number second moment closure without wall-reflection redistribution terms", *Proceedings, 11th Symposium on Turbulent Shear Flows*, Grenoble, France, Vol. 1, pp. 7-12:7-17.

Skåre, P.E. and Krogstad, P-Å, 1994, "A turbulent equilibrium boundary layer near separation", *J. Fluid Mech.*, Vol. 272, pp. 319-348.

Spalart, P.R., 1988, "Direct simulation of a turbulent boundary layer up to $R_\theta = 1410$", *J. Fluid Mech.*, Vol. 187, pp. 61-98.

Wallin, S., and Johansson A.V., 2000, "An explicit algebraic Reynolds stress model for incompressible and compressible flows", *J. Fluid Mech.*, Vol. 403, pp. 89-132.